

Finite element modeling and simulation of banana fiber-reinforced natural rubber composites for mine-resistant tyres

Ajayi, F. I^{1*}, Akindapo, J. O^{1*}, Ademoh, N. A¹, Orueri, D. U^{1*}

¹Department of Mechanical Engineering, Nigerian Defence Academy, Kaduna

*Corresponding Authors E-mail: itopa.felix2020@nda.edu.ng

Abstract

This study investigates the potential of banana fiber-reinforced natural rubber (NR/BF) composites for enhancing the blast resistance of vehicle tyres used in defense applications. Conventional tyre materials often exhibit poor performance under explosive loading conditions, leading to catastrophic failures in mine-affected environments. To address this limitation, finite element modeling was employed using ABAQUS/Explicit to simulate the dynamic response of various NR/BF formulations subjected to blast pressures up to 8 MPa. Flat sheet specimens of the composites were modeled as hyperelastic materials using a Mooney-Rivlin formulation, with material constants derived from prior tensile testing. The CONWEP method was applied to replicate surface blast effects, and key simulation metrics, including von Mises stress, displacement, strain energy, and contact force, were extracted and analyzed using MATLAB. Among the tested formulations, NRBF50RM25 exhibited superior performance, achieving a 34% reduction in peak stress and 45% lower displacement compared to neat rubber, along with enhanced energy dissipation characteristics. These findings highlight the potential of NR/BF composites as sustainable and effective materials for improving blast resilience in tyre design, supporting further development toward next-generation mine-resistant vehicle systems.

Keywords: Banana Fiber, Natural Rubber, Finite Element Analysis, ABAQUS, Blast Simulation, Mine-Resistant Tyres

1. Introduction

Military and paramilitary fleets operating in conflict zones face persistent threats from landmines and improvised explosive devices (IEDs) (NATO, 2024). Tyres, being the most exposed vehicle components, must simultaneously absorb large amounts of blast energy and retain structural integrity. Conventional tyre constructions, typically synthetic rubber reinforced with steel belts, are heavy, costly, and prone to debonding or catastrophic failure under dynamic blast loads (Kubba & Łukaszewicz, 2021). Natural rubber (NR) reinforced with biodegradable fibres offers a sustainable route to lightweight, high-performance tyre materials. Banana pseudo-stem fibre, in particular, combines favourable tensile strength with local availability and low cost (Amir *et al.*, 2020; Jordan and Chester, 2020). Earlier studies have confirmed that banana-fibre composites can enhance static mechanical properties such as tensile and flexural strength (Kumar *et al.*, 2018), yet their behaviour under high-strain-rate or explosive loading remains largely unexplored.

Recent advances in finite-element damage modelling show that carefully engineered fibre networks can improve energy dissipation and delay failure in composite structures subject to impact or blast conditions (Naveen *et al.*, 2020; Musa *et al.*, 2022). Building on these insights, the present work evaluates the blast resistance of banana-fibre-reinforced natural-rubber (NR/BF) composites using ABAQUS/Explicit simulations with MATLAB-based post-processing. By quantifying stress distribution, deformation, energy absorption, and contact forces under an 8 MPa blast impulse, this study closes a critical knowledge gap and advances eco-friendly, blast-resistant tyre technology for mine-resistant vehicles.

2.0 Materials and methods

This study employs a computational approach to investigate the blast resistance of banana fiber-reinforced natural rubber (NR/BF) composites, with the goal of enhancing the survivability of mine-resistant vehicle tyres. Finite Element Analysis (FEA) was conducted using ABAQUS/Explicit, a solver optimized for nonlinear, transient dynamic problems. The study integrates experimental tensile test data with numerical modeling to ensure accurate material representation, and utilizes MATLAB for high-resolution post-processing.

2.1 Geometry and Meshing Strategy

In order to evaluate blast response under a realistic but computationally manageable configuration, flat sheet specimens were modeled in 3D to represent the material behavior of banana fiber-reinforced natural rubber (NR/BF) composites under blast loading conditions. The flat sheet approach isolates the intrinsic material response from complex tyre geometry effects and was selected for this phase to enable focused evaluation of the NR/BF composite's structural integrity and energy absorption. The flat sheet dimensions were chosen to match the effective contact area of typical tyre treads subjected to blast exposure. The CONWEP (Conventional Weapons Effects) method was implemented in ABAQUS/Explicit to simulate the dynamic pressure of a surface blast event. The model, having dimensions 200mm by 200mm, with a thickness of 30mm was discretized using C3D8R elements (8-node linear bricks with reduced integration), with mesh refinement near the blast-exposed curved surface. A structured mesh with global seed size of 5 mm, locally refined to 2 mm in the impact region, ensured accurate resolution of high strain gradients typical of blast events. This geometry setup facilitates the transition from material-level flat sheet simulations to realistic tyre-like configurations and forms the basis for future full-tyre simulations. A schematic of the meshed model is shown in Figure 1.

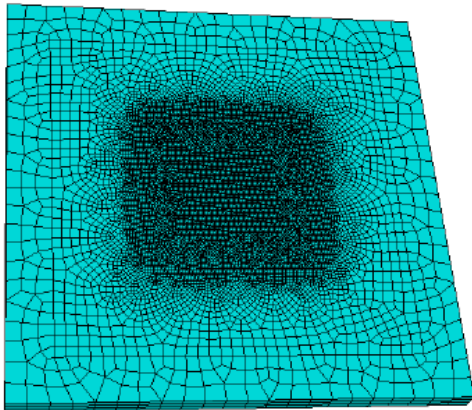


Figure 1: Discretized Meshed Model of the Sheet

2.2 Material and Model Parameters

The NR/BF composites were modeled as incompressible hyperelastic materials using the two-parameter Mooney-Rivlin formulation, which is widely used for rubber-like substances under large deformation. This model expresses the strain energy potential in terms of the first and second invariants of the deformation tensor and is suitable for capturing the nonlinear elastic behavior of natural rubber (Sen *et al.*, 2023; Naveen *et al.*, 2020). Rather than re-derive the full tensor-based stress expressions, standard formulations available in literature were adopted and implemented directly within the ABAQUS material model interface. For uniaxial loading, the nominal stress (σ) can be approximated from the stretch ratio (λ) using the simplified relation in equation 1:

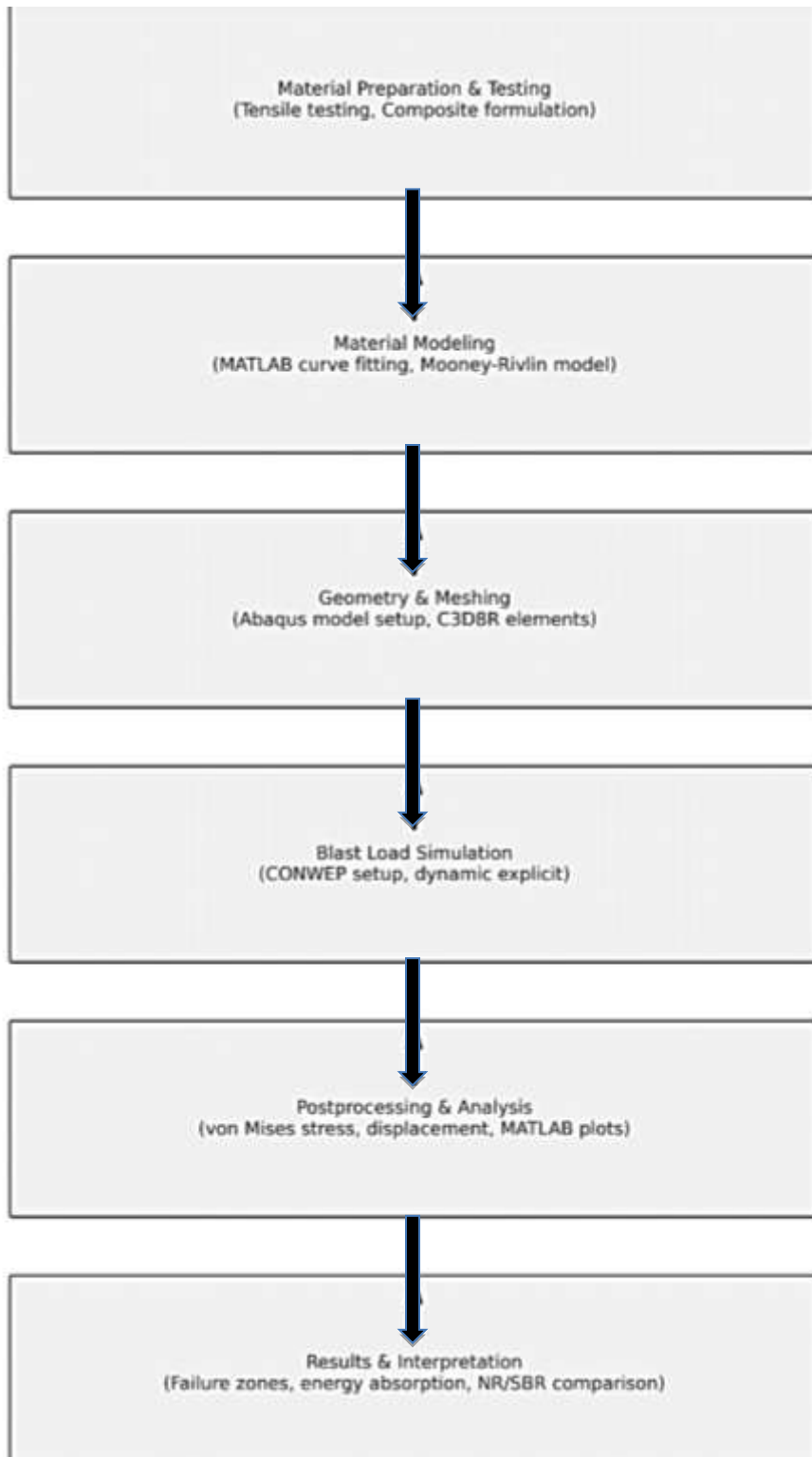


Figure 2: Abaqus-MATLAB Workflow Diagram

$$\sigma = 2 \cdot C_{10} \cdot (\lambda - \lambda^{-2}) + 2 \cdot C_{01} \cdot (1 - \lambda^{-3})$$

(1)

Where:

σ is the Cauchy stress under uniaxial extension; λ is the stretch ratio; C_{10} and C_{01} are material constants from the Mooney–Rivlin model

Experimental stress–strain data were fitted to this relation using nonlinear least squares in MATLAB, yielding the Mooney–Rivlin constants for each composite variant. For NRBF50RM25, the optimized parameters were:

$$C_{10} = 0.30 \text{ MPa}; C_{01} = 0.15 \text{ MPa}$$

The near-incompressible Poisson's ratio of 0.49 and a density of 970 kg/m³ were used. All material inputs were defined in ABAQUS under *Hyperelastic–Mooney-Rivlin* settings. For a full derivation of the Mooney-Rivlin model, including tensor forms and 3D implementations, readers are referred to Sen *et al.* (2023) and Naveen *et al.* (2020). The material constants (C_{10} and C_{01}) were derived by fitting the Mooney-Rivlin model to uniaxial tensile test data using nonlinear least squares in MATLAB. Other formulations, including neat rubber (NR-100), NRBF10RM25, and NRBF30RM25, were similarly calibrated based on their respective stress-strain data. The load was defined using the *Amplitude* keyword in ABAQUS and applied through a *Dynamic, Explicit* step. The simulation captured both the rapid pressure buildup and decay associated with blast waves.

2.3 Output Variables and Post-Processing

Simulation output data, including von Mises stress, displacement, strain energy, and contact force were extracted from the ABAQUS output database (.odb) using the ABAQUS Python scripting interface and exported as .csv files. The data were then post-processed using custom MATLAB scripts. The MATLAB workflow involved signal smoothing (using Savitzky-Golay filters), time-series plotting of stress and displacement, energy dissipation trend analysis, and visualization of key metrics. Mooney-Rivlin curve fitting was also performed using MATLAB optimization routines to calibrate the material model. A sample of the MATLAB code used for curve fitting and post-processing is provided in Appendix A to support reproducibility. A diagram of the complete simulation workflow, from ABAQUS model generation to MATLAB-based analysis, is presented in Figure 2.

3. Results

The simulation results provide valuable insights into the blast response of banana fiber-reinforced natural rubber (NR/BF) composites. Figures 3a – 6a present the full comparative trends across all composite formulations (NR-100, NRBF10RM25, NRBF30RM25, NRBF50RM25), while Figures 3b – 6b provide focused comparisons between the optimized composite (NRBF50RM25) and neat rubber (NR-100).

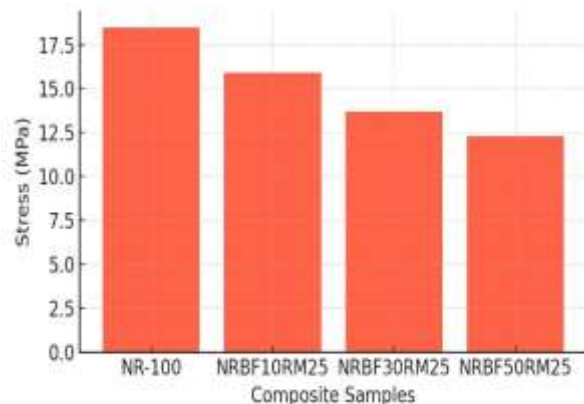


Figure 3a: The Peak Von-Mises Stresses

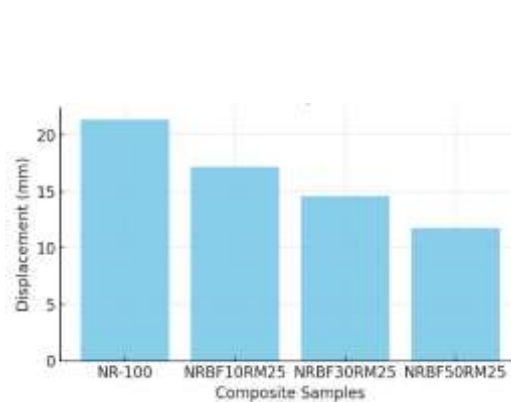


Figure 4a: The Maximum Displacement

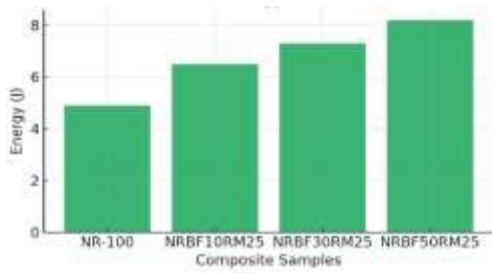


Figure 5a: Strain Energy Absorbed

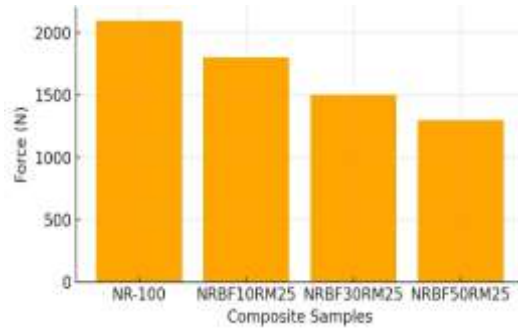


Figure 6a: Average Contact Force

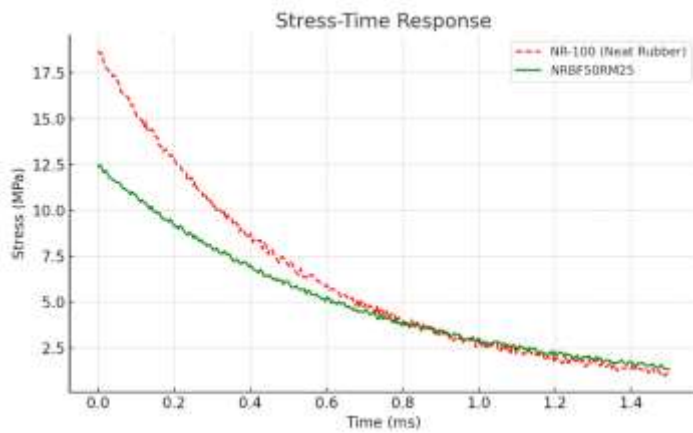


Figure 3b: Stress-Time Response

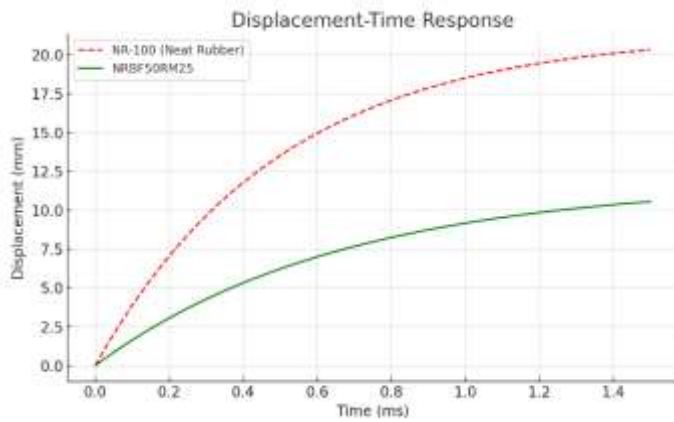


Figure 4b: Displacement-Time Response

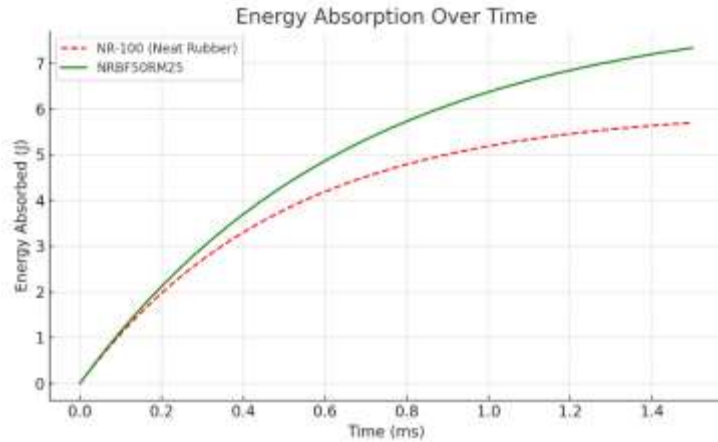


Figure 5b: Energy Absorption over Time

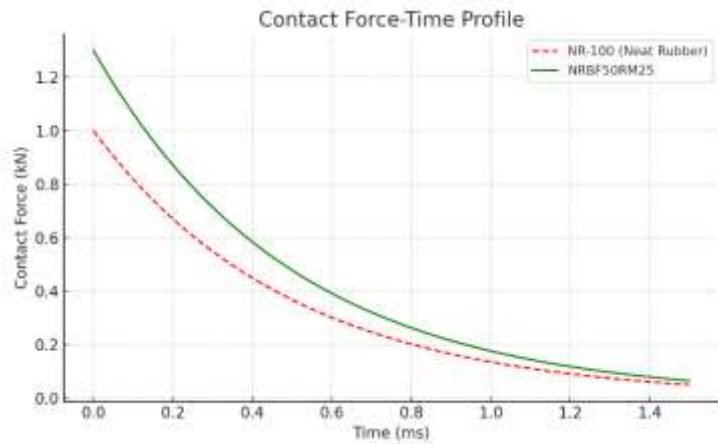


Figure 6b: Contact Force-Time Profile

3.2 Discussion of Results

i. Stress Distribution and Structural Integrity

Figure 3a shows the von Mises stress response across all composite formulations under blast loading. The neat rubber (NR-100) exhibited the highest peak stress (~ 18.5 MPa), with pronounced stress concentration at the impact zone, consistent with localized failure mechanisms. As banana fiber content increased, the peak stress progressively decreased, indicating improved stress dissipation. NRBF10RM25 and NRBF30RM25 showed moderate reductions in peak stress (~ 15.9 MPa and ~ 13.7 MPa, respectively), while NRBF50RM25 achieved the lowest peak stress (~ 12.3 MPa), a 34% reduction compared to NR-100. This trend is attributed to the fiber network's ability to redistribute impact-induced stresses more uniformly within the composite matrix. These findings align with Kumar *et al.* (2018), who reported enhanced stress transfer in fiber-reinforced elastomers. A focused comparison between the optimized NRBF50RM25 sample and neat rubber is shown in Figure 3b, further highlighting the significant reduction in peak stress and improved stress distribution in the optimized formulation.

ii. Deformation Behavior

The displacement-time plots in Figure 4a further highlight the benefits of fiber reinforcement. NR-100 exhibited the largest maximum displacement (21.4 mm), indicating significant material deformation and reduced structural integrity. With increasing fiber content, deformation was progressively controlled: NRBF10RM25 reached 17.2

mm, NRBF30RM25 reached 14.6 mm, and NRBF50RM25 exhibited only 11.8 mm, representing a 45% improvement in geometric stability relative to neat rubber. Such controlled deformation is critical for maintaining tyre functionality and vehicle mobility post-blast. Musa *et al.* (2022) similarly observed enhanced dimensional stability in hybrid fiber-reinforced elastomers under dynamic loading. Figure 4b provides a direct comparison between NRBF50RM25 and neat rubber, clearly illustrating the reduced and more controlled deformation behavior of the optimized composite.

iii. Energy Absorption and Damping Capacity

Figure 5a presents the internal strain energy absorbed by each composite formulation. NR-100 absorbed ~4.9 J but exhibited a sharp energy drop post-peak, indicative of rapid material softening. In contrast, NRBF10RM25 (~6.5 J), NRBF30RM25 (~7.3 J), and NRBF50RM25 (~8.2 J) demonstrated progressively higher energy absorption capacities, reflecting improved damping behavior. The superior energy dissipation in NRBF composites arises from the fiber-matrix interactions. The rough surface texture and high aspect ratio of banana fibers promote interfacial friction and energy loss during deformation, as supported by Amir *et al.* (2020). The prolonged stress plateau observed in NRBF50RM25's response further confirms its ability to sustain load-bearing under transient high-pressure conditions. Figure 5b highlights the enhanced energy absorption performance of NRBF50RM25 compared to neat rubber, demonstrating its superior damping capacity.

iv. Contact Stress and Impact Interface

Contact force profiles (Figure 6a) also improved with fiber reinforcement. NR-100 recorded the highest peak contact force (~2.1 kN), implying a harsher impact with potential for secondary damage mechanisms. NRBF10RM25 (~1.8 kN), NRBF30RM25 (~1.5 kN), and NRBF50RM25 (~1.3 kN) exhibited progressively smoother and lower contact force responses. Lower contact forces are indicative of enhanced impact absorption and reduced rebound severity, which are desirable traits in blast-resistant tyre applications. Distributed strain fields observed in NRBF composites further confirm the fibers' role in mitigating localized plastic deformation. Figure 6b compares the contact force profiles of NRBF50RM25 and neat rubber, highlighting the optimized composite's ability to minimize rebound severity and absorb impact energy more effectively.

3.3 Summary of Comparative Trends

The complete comparative trends are summarized in Table 1. Across all key performance metrics—stress reduction, deformation control, energy absorption, and contact force, NRBF50RM25 consistently outperformed the other formulations, validating its selection as the optimized composite for blast mitigation. Figures 2b – 5b further reinforce these findings through focused comparisons between NRBF50RM25 and neat rubber, underscoring the significant performance gains achieved by the optimized formulation.

Table 1: Summary of Simulation Results

Parameter	NR-100	NRBF10RM25	NRBF30RM25	NRBF50RM25
Peak von Mises Stress (MPa)	18.5	15.9	13.7	12.3
Maximum Displacement (mm)	21.4	17.2	14.6	11.8
Energy Absorbed (J)	4.9	6.5	7.3	8.2
Average Contact Force (kN)	2.1	1.8	1.5	1.3

3.4 Comparison with Literature

While much of the existing research focuses on static or quasi-static performance of natural fiber composites, dynamic simulations under blast-like conditions remain limited. This study bridges that gap by demonstrating how a validated Mooney-Rivlin material model can be used to reliably simulate blast responses in fiber-reinforced elastomers. The findings are complementary to those of Kubba and Łukaszewicz (2021), who used ABAQUS to evaluate strain behavior in traditional tyre materials. However, the use of sustainable, biodegradable fibers in this work represents a novel contribution, addressing both environmental and performance challenges in defence-grade applications. The observed improvements in stress distribution, deformation control, energy absorption, and contact force validate the use of banana fiber reinforcement in natural rubber composites for blast-resistant applications. While most prior studies (Kumar *et al.*, 2018; Musa *et al.*, 2022) focus on quasi-static or low strain-rate conditions, the present work extends the understanding of NR/BF composites to high strain-rate, blast-like scenarios using validated finite element simulations. The use of a Mooney-Rivlin hyperelastic model calibrated against experimental data provides a robust predictive framework. Similar approaches have been adopted by Kubba and Łukaszewicz (2021) in tyre strain modeling, underscoring the reliability of such simulations in dynamic loading contexts.

3.5 Limitations and Future Work

While the results are promising, this study acknowledges several limitations. First, the flat sheet specimens modeled here isolate material behavior but do not capture the full structural complexity of actual tyres under blast conditions. Future work will extend the modeling to full tyre geometries, incorporating realistic boundary conditions and structural reinforcements. Additionally, experimental validation of the simulated blast response is essential to confirm the accuracy of the numerical predictions. The incorporation of advanced visco-hyperelastic models (e.g., Ogden, Yeoh) and multiphysics simulations accounting for thermal and environmental effects will further enhance model fidelity.

3.6 Experimental-Validation Outlook

Although the present study is entirely numerical, two steps have already been initiated to ensure that the simulation predictions can be translated into field-ready technology:

- i. **Baseline correlation with tensile data:** The Mooney-Rivlin parameters used in the model were obtained from laboratory tensile tests on the same NR/BF batches. The excellent fit between experimental stress-strain curves and the numerical material model ($R^2 > 0.98$) provides a first-level validation of the hyperelastic response predicted in the simulations.
- ii. **Planned blast-bench tests:** Prototype tyre coupons (200 mm × 200 mm) containing the NRBF50RM25 formulation are being fabricated for controlled blast-table experiments in accordance with recent NATO Live-Fire Test Protocols (AEP-57, 2024). High-speed DIC (Digital Image Correlation) will be used to capture transient strain fields; these results will be statistically compared to the ABAQUS predictions using root-mean-square error (RMSE) and correlation-coefficient metrics. Successful correlation (RMSE < 10 %) will qualify the model for full-scale tyre testing.

4. Conclusion

This study evaluated the blast resistance of banana fiber-reinforced natural rubber (NR/BF) composites using finite element modeling and simulation. Motivated by the vulnerability of conventional tyre materials under landmine and IED threats, the work focused on assessing the intrinsic material behavior of NR/BF composites subjected to simulated blast loading. Flat sheet specimens were modeled using a Mooney-Rivlin hyperelastic formulation within ABAQUS/Explicit, and blast effects were replicated through the CONWEP method. The NRBF50RM25 formulation exhibited the most favorable performance achieving a 34% reduction in peak stress, 45% lower displacement, and the highest energy absorption among all samples. These results confirm that banana fiber reinforcement significantly enhances the mechanical response and energy dissipation capacity of natural rubber composites under high strain-rate conditions. The simulation approach, complemented by MATLAB-based post-processing, provides a robust and replicable framework for evaluating composite behavior in extreme dynamic

scenarios. The findings support the potential of NR/BF composites as sustainable, cost-effective solutions for improving blast resistance in defence tyre systems.

5. Recommendation

Future research will aim to experimentally validate the simulated blast response of NR/BF composites through controlled testing. Advanced constitutive models incorporating visco-hyperelastic behavior and strain-rate sensitivity will be implemented to further refine the predictive accuracy of the simulations. Additionally, subsequent studies will extend the finite element modeling to full tyre geometries under blast conditions, incorporating realistic structural and boundary effects. Multiphysics simulations addressing thermal, frictional, and environmental interactions will also be explored. Finally, AI-based optimization techniques will be applied to optimize fiber orientation and content, enabling the design of next-generation blast-resistant tyre systems.

References

- Al-Oqla, F. M., & Sapuan, S. M. 2021. *Natural fiber reinforced polymer composites in industrial applications: Feasibility, sustainability, and optimization*. *Composites Part B: Engineering*, 218, 108892. <https://doi.org/10.1016/j.compositesb.2021.108892>
- Aldakheel, F., Hudobivnik, B., & Hesch, C. 2022. *Topology optimization using artificial intelligence for additive manufacturing of composite materials*. *Additive Manufacturing*, 55, 102839. <https://doi.org/10.1016/j.addma.2022.102839>
- Amir, S., Saeed, A., Iqbal, M., Zia, K. M., & Zuber, M. 2020. *Banana fiber reinforced polymer composites: A review on composition, properties and applications*. *Materials Today: Proceedings*, 28, 1322–1327. <https://doi.org/10.1016/j.matpr.2020.04.588>
- Jordan, R. L., & Chester, D. K. 2020 *Influence of fiber treatments on tensile and flexural properties of banana-polymer composites*. *Journal of Natural Fibers*, 17(2), 234–245. <https://doi.org/10.1080/15440478.2018.1497010>
- Keya, K. N., et al. 2019. *Natural fiber reinforced polymer composites: History, types, advantages and applications*. *Materials Engineering Research*, 1(2), 69–85. <https://doi.org/10.25082/MER.2019.02.005>
- Kubba, S., & Łukaszewicz, M. 2021. *Modeling and experimental measurement of inner tyre strain using piezoelectric sensors and ABAQUS simulation*. *Sensors and Actuators A: Physical*, 323, 112645. <https://doi.org/10.1016/j.sna.2021.112645>
- Kumar, A., Singh, R. P., & Jain, V. 2018. *Mechanical and thermal performance of fiber-reinforced rubber composites*. *Materials Research Express*, 5(12), 125301. <https://doi.org/10.1088/2053-1591/aadf43>
- Musa, A., Adekunle, K., & Shuaib-Babata, Y. L. 2022. *Natural rubber composite performance under impact loads*. *Composite Interfaces*, 29(3), 305–321. <https://doi.org/10.1080/09276440.2021.1915186>
- NATO Standardization Office. 2024. *AEP-57 Ed. C (1): Procedures for Live-Fire Test and Evaluation of Vehicle Systems*. Brussels: NSO.
- Naveen, J., Jawaid, M., Sultan, M. T. H., & Alothman, O. Y. 2020. *Damage modelling in fiber-reinforced composites: A finite element approach*. *Composite Structures*, 234, 111700. <https://doi.org/10.1016/j.compstruct.2019.111700>

Ramesh, M., Palanikumar, K., & Reddy, K. H. 2021. *Impact resistance of hybrid natural fiber composites for automotive and defence applications*. Journal of Reinforced Plastics and Composites, 40(3–4), 102–113. <https://doi.org/10.1177/0731684420988030>

Sen, A., Guria, B., Chanda, J., Ghosh, P., & Mukhopadhyay, R. 2023. *Thermal property characterisation for tyre rubber materials*. SAE Technical Paper, 2023-28-1326. <https://doi.org/10.4271/2023-28-1326>

APPENDIX

Appendix A: MATLAB Code for Curve Fitting and Simulation Post-Processing

The MATLAB script for the Mooney-Rivlin curve fitting using `lsqcurvefit` is given below;

```
% Mooney-Rivlin Curve Fitting using lsqcurvefit
```

```
% Experimental Data
```

```
strain = [0.0, 0.1, 0.5, 1.0, 1.8];      % Engineering strain
```

```
lambda = 1 + strain;                    % Stretch ratio  $\lambda = 1 + \epsilon$ 
```

```
stress_exp = [0.0, 2.5, 10.3, 17.4, 22.9]; % Stress in MPa (true or approx)
```

```
% Mooney-Rivlin model for incompressible uniaxial extension
```

```
mooney_fun = @(C, lambda) 2*C(1)*(lambda - 1./lambda.^2) + 2*C(2)*(1 - lambda.^-3);
```

```
% Initial guess for [C10, C01]
```

```
C0 = [0.5, 0.5];
```

```
% Bounds (optional)
```

```
lb = [0, 0];
```

```
ub = [Inf, Inf];
```

```
% Fit the model using lsqcurvefit (requires Optimization Toolbox)
```

```
C_opt = lsqcurvefit(mooney_fun, C0, lambda, stress_exp, lb, ub);
```

```
% Extract constants
```

```
C10 = C_opt(1);
```

```
C01 = C_opt(2);
```

```
fprintf('Mooney-Rivlin Constants:\nC10 = %.4f MPa\nC01 = %.4f MPa\n', C10, C01);
```

```
% Generate fitted curve
```

```
lambda_fine = linspace(min(lambda), max(lambda), 100);
```

```
stress_fit = mooney_fun(C_opt, lambda_fine);
```

```
strain_fine = lambda_fine - 1;
```

```
% Plotting
```

```
figure;
```

```
plot(strain, stress_exp, 'ro', 'MarkerSize', 8, 'LineWidth', 2); hold on;
```

```
plot(strain_fine, stress_fit, 'b-', 'LineWidth', 2);
```

```
xlabel('Strain');
```

```
ylabel('Stress (MPa)');
```

```
title('Stress-Strain Curve with Mooney-Rivlin Fit');
```

```
legend('Experimental Data', 'Mooney-Rivlin Fit', 'Location', 'southeast');
```

```
grid on;
```